Journal of Cancer Therapy, 2014, 5, 1388-1398
Published Online December 2014 in SciRes. http://www.scirp.org/journal/jct
http://dx.doi.org/10.4236/jct.2014.514140

Scientific Research

Deterministic Parsing Model of the Compound Biological Effectiveness (*CBE*) Factor for Intracellular ^{10}Boron Distribution in Boron Neutron Capture Therapy

Shintaro Ishiyama

Quantum Beam Science Directorate, Japan Atomic Energy Agency, Naka-gun, Japan
Email: ishiyama.shintaro@jaea.go.jp

Received 20 September 2014; revised 18 October 2014; accepted 14 November 2014

Academic Editor: Suresh Rana, ProCure Proton Therapy Center, USA

Abstract

Purpose: In defining the biological effects of the ^{10}B(n, α)^{7}Li neutron capture reaction, we have previously developed a deterministic parsing model to determine the Compound Biological Effectiveness (*CBE*) factor in Borono-Phenyl-Alanine (*BPA*)-mediated Boron Neutron Capture Therapy (*BNCT*). In present paper, we demonstrate that the *CBE* factor is directly and unambiguously derivable by the new formula for any case of intracellular ^{10}Boron (^{10}B) distribution, which is founded on this model for tissues and tumor. Method: To determine the *CBE* factor, we derive the following new calculation formula founded on the deterministic parsing model with three constants, CBE_0, F, n and the eigen value N_{th}/N_{max}.

$$CBE = CBE_0 + \frac{F}{2}\left(1-\left(\frac{N_{th}}{N_{max}}\right)^{\frac{1}{n}}\right)\left\{2-\left(\frac{N_{th}}{N_{max}}\right)^{\frac{2}{n}}+\left(\frac{N_{th}}{N_{max}}\right)^{\frac{1}{n}}\right\} \quad 0<\frac{N_{th}}{N_{max}}<1$$

where, N_{th} and N_{max} are the threshold value of boron concentration of N and saturation boron density in tissues and tumor. In order to determine these constants and the eigen values, iterative calculation technique was employed for the *CEB* factor and N_{max} data set previously reported. Results and Conclusion: From the iterative calculation results, it is clear that the calculated *CBE* factor values obtained are almost identical to the original *CBE* factors and there is a good correlation between the original *CBE* factors and N_{th}/N_{max}, when CBE_0, F and n are given as 0.5, 8 and 3, respectively. These constants provide a better understanding of different types of intracellular ^{10}B distribution.

How to cite this paper: Ishiyama, S. (2014) Deterministic Parsing Model of the Compound Biological Effectiveness (*CBE*) Factor for Intracellular ^{10}Boron Distribution in Boron Neutron Capture Therapy. *Journal of Cancer Therapy*, **5**, 1388-1398.
http://dx.doi.org/10.4236/jct.2014.514140

Keywords

Boron Neutron Capture Therapy, Compound Biological Effectiveness, Borono-Phenyl-Alanine, Tumor, $^{10}B(n, \alpha)^{7}Li$

1. Introduction

Many types of pilot innovative accelerator-based neutron source for neutron capture therapy with lithium target were designed [1]-[3] and many inventions for the progressive power run-up were reported [4] [5]. In Japan, implemented deployment of accelerator-driven neutron source for Boron Neutron Capture Therapy (*BNCT*) is scheduled in 2014 in National Cancer Center, of which system was designed with the production of neutrons via threshold $^{7}Li(p, n)^{7}Be$ reaction at 25 kW proton beam with energy of 2.5 MeV, which was designed to dovetail the narrow peak band resonance of lithium target and started its installation at middle of 2013. This *BNCT* device is expected to offer the potential for achieving the objects of which any treatment capable of sterilizing the primary tumor locally will result in a high probability of cure.

BNCT is a targeted radio-therapeutic modality used for the treatment of brain tumors and melanoma and a bimodal approach to cancer therapy. Before *BNCT*, Boron-10(^{10}B)-enriched compounds are used to deliver ^{10}B to tumors. Once tumor uptake of a given boron delivery agent relative to the surrounding normal tissues and blood has been maximized and then irradiation with low-energy neutron takes place. An alternative boron delivery agent, p-borononphenylalaine (*BPA*) instead of administration of the boron delivery agent borocaptate sodium (BSH), is being used together with mode deeply penetrating epithermal neutron beam [6]. *BNCT* was extensively reviewed in two recent articles [7] [8] and the targeting effectiveness of *BNCT* was dependent upon the preferential delivery of ^{10}B to the primary tumor and its metastatic spread.

In defining the biological effects of the $^{10}B(p, \alpha)^{7}Li$ neutron capture reaction relative to photons, the term compound biological effectiveness (*CBE*) factor was used as an alternative to *RBE*. Calculation of the *CBE* factor is similar to that of the *RBE* factor [9]. Equating the X-ray ED_{50} dose with a BNC dose (beam + BSH) that gives the same end point of a 50% incident of ulceration produces the following equation:

The *CBE* factor = [(X-ray ED_{50}) − (thermal beam component of ED_{50} × RBE]/$^{10}B(p, \alpha)^{7}Li$ component of ED_{50}.

Recently, the *CBE* factors concerning to tumor, skin lung, liver [10] [11], heart [12] and oral mucosal tissues [13] were reported and prospect of actually using *BNCT* for the patients has been developing under the right circumstances. However, there is no theoretical unified explanation of the *CBE* factors for normal tissues and tumor, despite the fact that significance of high precision of the *CBE* factor evaluation is requested for the patients.

The purpose of the present investigation was to demonstrate the deterministic parsing model of the *CBE* factor for intracellular ^{10}B distribution and discover the unified methodology for the evaluation of the *CBE* factors for normal tissues and tumor in *BNCT*.

2. Materials and Methods

2.1. ^{10}B Concentration and the CEB Factors of *BPA*

As for the *CBE* factor and boron concentration data set of *BPA* previously obtained in biological test for normal tumor, skin lung, liver [10] [11], heart [12] and oral mucosal tissues [13] [14], we can classify these data into two main groups, tumor and normal tissue and no relationship between $N_{B\text{-}max}$ and *CBE* factor was not found in normal tissue group (**Table 1**, **Figure 1**).

2.2. Mathematical Analysis Model for the *CBE* Factor

2.2.1. Definition of the Duplicate Volume of the α Range and Proximity of Boron Atoms

Thermal neutrons or epithermal neutrons, which become thermalized at depth in tissue, are captured by ^{10}B atoms, with the resultant fission reaction producing α-particles and lithium-7 (^{7}Li) ions in *BNCT*.

These particles have a limited range of <9 μm in tissue. Thus, it is possible to selectively irradiate a tumor with high Linear Energy Transfer (LET) radiation, while sparing the adjacent normal tissues, theoretically. ^{10}BPA is designed to be selectively spatially-integrated into the tumor cells and boron atoms are distributed in a

Table 1. The data set of the *CBE* factor and N_{max} for normal tissues and tumour obtained in the case of *BPA* administration.

No.	Tissue	$N_{B\text{-}max}$ (μg/g)	*CBE* Factor
1[1)]	Tumor	72	3.8
2[2)]	Normal skin tissue	28.8	2.5
3[3)]	Normal brain tissue	20	1.34
4[4)]	Normal oral mucosal tissue	21.5	4.87
5[5)]	Normal liver tissue	24	4.25
6[6)]	Normal lung tissue	24	2.3
7[7)]	Normal heart tissue	24	1.35

[1)]Fukuda *et al*., 1994, [2)]Kiger *et al*., 2008, [3)]Suzuki *et al*., 2000, [4)-7)]Morris *et al*., 1997 with *BPA* experiments of mice.

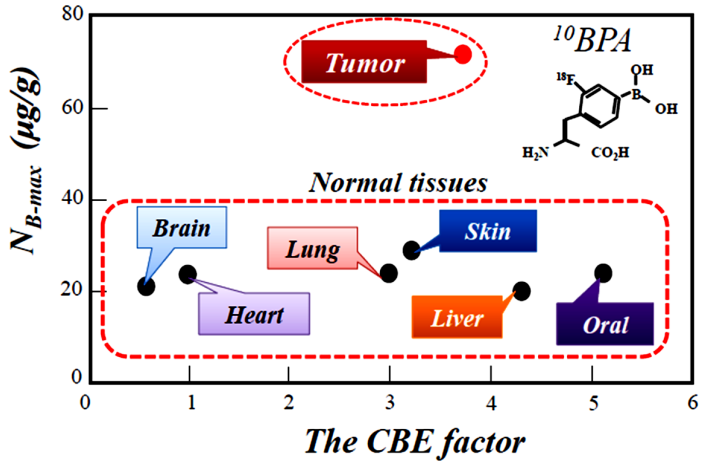

Figure 1. The relationship between the *CBE* factor and N_{max} in the case of ^{10}*BPA* administration.

cell and to damage these area due to $^{10}B(n, \alpha)^{7}Li$ reaction (**Figure 2**).

Distance r_0 and $2r$ were defined as α range and distance between boron atoms in the figure. There are two conditions of boron atom exists beyond the α range ($r_0 \le r$) (**Figure 2(b)**) and boron atoms within α range ($r_0 > r$) mainly investigated in present study (**Figure 2(c)**).

In the case study of (c), there is the duplicate volume V_d, where is exposed under duplicated irradiation by α particles from the both side of boron atoms.

Here, we postulate the correlation between the *CBE* factor and V_d in the case of (c) as;

$$CBE \propto F \cdot V_d \tag{1}$$

where proximity F is the number of boron atoms surrounding to in the centered born atom and the geometric duplicated volume of V_d is given by the formula of the volume of spherical cap with r_0 and r;

$$V_d = \frac{2}{3}\tau r_0^3\left(1-\frac{r}{r_0}\right)\left\{2-\left(\left(\frac{r}{r_0}\right)^2+\frac{r}{r_0}\right)\right\} \tag{2}$$

Here, V_d is normalized by the volume $V_0\left(=4/3\pi r_0^3\right)$ given as the α range volume, and the normalized duplicate volume V_{dnor} can be expressed as the ratio of V_d and V_0 (**Figure 3**).

$$V_{dnol} = \frac{V_d}{V_0} = \frac{1}{2}\left(1-\frac{r}{r_0}\right)\left\{2-\left(\left(\frac{r}{r_0}\right)^2+\frac{r}{r_0}\right)\right\} \tag{3}$$

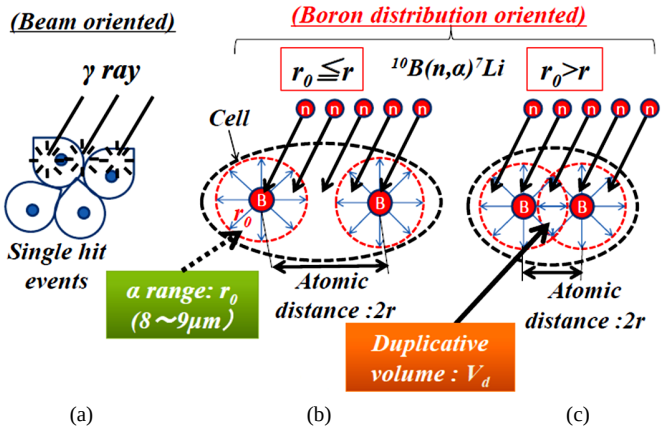

Figure 2. Images of irradiation damage and its effective area caused by (a) γ ray, α particle irradiation due to $^{10}B(n, \alpha)^7Li$ reaction in the (b) access distance ($r_0 < r$) and (c) distance of closet approach ($r_0 > r$) between boron atoms.

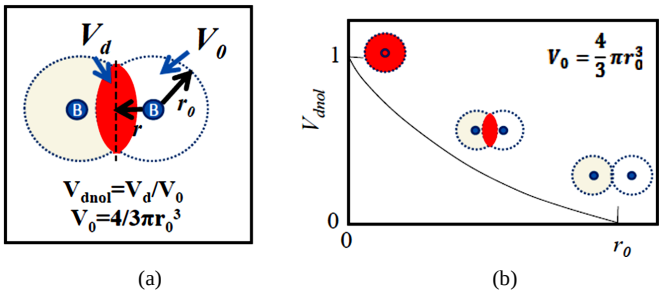

Figure 3. Definition of (a) the duplicate volume of spherical cap of two α range volumes and (b) the change in the duplication volune as a function of the distance between boron atoms.

2.2.2. Space Factor *n*

After *BPA* administration, bio-distribution of ^{10}B atoms is provided into a cell (**Figure 4**) and boron atoms become closer with each other, but exist beyond α range in the case of **Figure 4(a)**.

In contrast to this case, boron atoms are spatially-integrated selectively in a cell as *BPA* administration proceeds, very high dose of boron concentration is achieved as shown in the **Figure 4(b)** and **Figure 4(c)**.

Therefore, it can be assumed that there is a relationship between boron concentration N and distance of boron atoms r within the limited volume and space of cells (20 - 200 μm);

$$r \propto 1/N \tag{4}$$

Thus, we expressed the relationship between normalized boron concentration N/N_{th} and normalized r/r_0 here as;

$$r/r_0 = \left(N_{th}/N\right)^{1/n} \tag{5}$$

where n is the space factor (=1, 2, 3) and N_{th} is the threshold of N.

From Equation (3) and (5), V_{dnol} in Equation (3) is replaced as;

$$V_{dnol} = \frac{1}{2}\left(1-\left(\frac{N_{th}}{N}\right)^{\frac{1}{n}}\right)\left\{2-\left(\frac{N_{th}}{N}\right)^{\frac{2}{n}}+\left(\frac{N_{th}}{N}\right)^{\frac{1}{n}}\right\} \tag{6}$$

2.2.3. Definition of the Deterministic Parsing *CBE* Factor Model

From Equations (1) and (6), we defined the deterministic parsing *CBE* factor model as;

$$CBE = CBE_0 + \frac{F}{2}\left(1-\left(\frac{N_{th}}{N_{max}}\right)^{\frac{1}{n}}\right)\left\{2-\left(\frac{N_{th}}{N_{max}}\right)^{\frac{2}{n}}+\left(\frac{N_{th}}{N_{max}}\right)^{\frac{1}{n}}\right\} \quad (7)$$

$$0 < \frac{N_{th}}{N_{max}} < 1 \quad (8)$$

where N_{max} is the saturated boron concentration mentioned-below and CBE_0, F and n are constants.

2.3. Theoretical Calculation Method and Its Procedure

Iterative calculation technique was applied to obtain constants CBE_0, F, n and the eigen values of N_{th} in Equation (7) for each cases (Figure 5).

We started iteration calculation with data set of (N_{max}, CBE) in Table 1 and arbitrary values of CBE_0, F and n in Equation (7) to obtain N_{th} value, where n was give as a number of 1 - 3 (process (a)). With the calculation results of N_{th} value obtained in each cases, first data set was rewritten as (N_{th}/N_{max}, CBE) and calculated again to optimize constants CBE_0 and F in the equation by least square method with these new data set (process (b)). Then, these calculation processes were terminated when the identical calculated CBE values to the original CBE values were obtained.

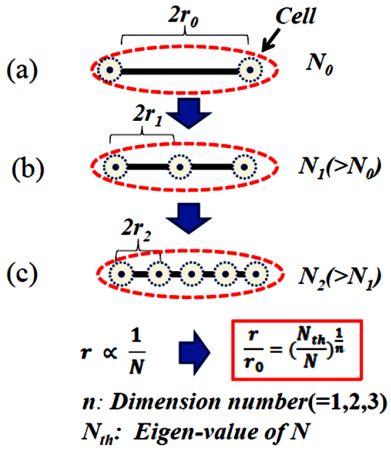

Figure 4. Concentration process of boron atoms into cell after *BPA* administration.

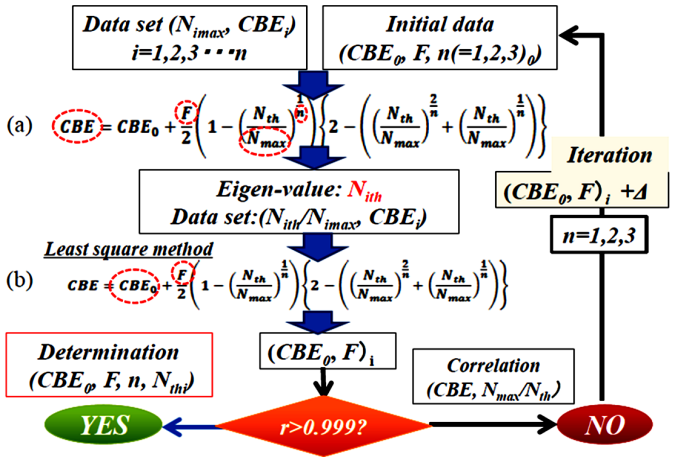

Figure 5. Iterative calculation process to obtain constants CBE_0, F, n and eigen value N_{th} in Equation (7).

3. Results and Discussions

3.1. The *CBE* Factor Model for Normal Tissues and Tumor

The calculated *CBE* values obtained by the above-mentioned theoretical calculation procedure are listed with the original *CBE* values in the table (Table 2).

According to Table 2, it was found that the calculated *CBE* values obtained are almost identical to the original *CBE* factors, when CBE_0, F and n are selected as 0.5, 8 and 3, respectively. Threshold values, N_{th} given by this calculation method are also listed for all cases in this table.

With these results, the original *CBE* factors are plotted as a function of the ratio, N_{th}/N_{max} and the solid line in this figure was provided by Equation (7) (Figure 6).

It is clear that there is a good correlation between the original *CBE* factors and N_{th}/N_{max} for all cases including tumor and it is concluded that the original *CBE* factors can be well expressed by Equation (7) with a parameter N_{th}/N_{max}.

Here we emphasise that the a threshold N_{th} exists to surmount the potential barrier of *BPA* concentration, for which less than N_{th}, remarkable damages by α particles cannot occur in *BNCT* [15].

3.2. Definition of Three Constants in the *CBE* Factor Model

3.2.1. Determination of the *CBE* Factor Depend on Boron Dose Level

The CBE_0 was defined as a intercept constant in Equation (7) and the *CBE* factor is given by CBE_0 value, which is determined as 0.5 for each intracellular distribution patterns (Figure 7).

Table 2. The results of iterative calculation of the *CBE* factor model presented in Equation (7).

No.	Tissue	N_{max} (μg/g)	N_{th} (μg/g)	*CBE* Factor	*CBE* (Calc.)	N_{th}/N_{max}
1	Tumor	72	8.71	3.8	3.81	0.121
2	Normal skin tissue	28.8	7.2	2.5	2.5	0.25
3	Normal brain tissue	20	9.3	1.34	1.35	0.465
4	Normal oral mucosal tissue	21.5	1.27	4.87	4.87	0.059
5	Normal liver tissue	24	2.21	4.25	4.25	0.092
6	Normal lung tissue	24	6.67	2.3	2.31	0.278
7	Normal heart tissue	24	11.14	1.35	1.35	0.464

$$CBE = 0.5 + \frac{8}{0}\left(1 - \left(\frac{N_{th}}{N_{max}}\right)^{\frac{1}{3}}\right)\left\{2 - \left(\frac{N_{th}}{N_{max}}\right)^{\frac{2}{3}} + \left(\frac{N_{th}}{N_{max}}\right)^{\frac{1}{3}}\right\}.$$

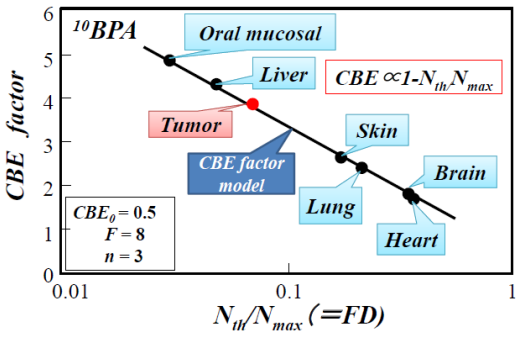

Figure 6. Deterministic parsing Model for the *CBE* factor with N_{th}/N_{max}.

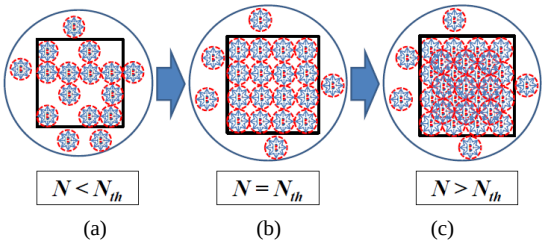

Figure 7. The *CBE* factor defined by CBE_0 constant in the cases of intracellular distribution of boron. (a) $r < r_0$; (b) $r = r_0$; (c) $r > r_0$.

In the figure, pattern a) is correspondent to lower boron concentration and boron atoms are distributed in a cell in heterogeneous condition. This condition can be defined in the case of $r > r_0$ in **Figure 2(b)** and each boron atom induces irradiation damages individually and significant damage is not expected because of lack of boron concentration in the affected area. As *BPA* administration proceeding, born concentration increases to the level of conditions b) and c) in the figure. The condition b) is homogeneous and critical case of $r = r_0$, in which boron dose N reaches to the threshold value N_{th} ($N = N_{th}$). In both cases of a) and b), the *CBE* factors are expected to be small value and given as constant level of CBE_0.

In contrast with these conditions, the condition c) is homogeneous over-packed case and correspond to $r < r_0$ ($N > N_{th}$) in **Figure 2(c)**. In this case, the *CBE* factor can be expressed by boron concentration N in Equation (7).

Therefore, the *CBE* factor can be defined by CBE_0 as following;

$$CBE = \begin{cases} 0.5, \& N < N_{\text{th}} \\ 0.5 + \dfrac{F}{2} * V_{dnol}, \& N \geq N_{\text{th}} \end{cases} \tag{9}$$

3.2.2. Sterically-Oriented Intracellular Distribution of Boron Atom

There are many types of sterically congested mode of ^{10}B atom distribution (**Figure 8**). Here, confront factor F in Equation (7) is defined as a sterically-oriented number of boron atoms surrounding center boron atom and is given as 8 in previous caption (2.1).

$$F = 8 \tag{10}$$

This result indicates that the data case in present study is corresponding to octahedron type and 8 boron atoms confronted to the center boron atom (**Figure 8(d)**).

Higher mode pattern also suggests a higher level of boron concentration under surgically observation and it is interest that proximity F informs sterically-oriented intracellular distribution of boron atom concentrated in the affected area.

3.2.3. Intracellular Cubic Array of Boron Atom

To define the relationship between the distance between boron atoms in a limited cell space, space factor n was adopted in Equation (5). There are allowable three patterns of space factor under the Equation (5) (**Figure 9**).

The space factor n = 1, 2 and 3 addresses liner, planar and stereo type cubic array, respectively. The space factor n is calculated as 3 in caption (2.1), this fact indicates that high level of boron concentration are achieved by stereo type cubic array formed after *BPA* administration in normal tissues and tumor cases.

$$n = 3 \tag{11}$$

The space factor n suggests cubic array structural extension of intracellular boron concentration, whereas F implied sterically-oriented intracellular proximity above-mentioned.

Two of these constant F and n are very important parameters to well-understanding boron concentration in normal tissues and tumor and to determine the effectiveness of *BNCT*.

3.3. Application of the *CBE* Factor Model for Human Brain Tumor

It is evident that the *CBE* factors for *BPA*, calculated using Equation (7) are the almost same values with those

obtained in previous animal experiments [10]-[13] and well expressed without distinction of tissues and tumor. Considered overall, the *CBE* factor is given as a function of boron concentration ratio, N_{th}/N_{max}.

In this section, we applied this calculation method to estimate the *CBE* factors for many types of human brain tumor.

Imahori reported dynamic PET analysis of 33 brain tumor patients contained of AII (8 patients), AIII (11) and GBM (14 Glio Blastoma Multiforme) [16] and presented typical change in ^{10}B concentration of blood, brain tumor and normal brain measured by dynamical PET technique during L-*BPA*-18F administration (**Figure 10**).

To determine the *CBE* factor, the values of N_{th} and N_{max} can be derived from the points on these typical dynamic PET curves. The N_{th} values were determined at the intersection points of two of fitting lines on ^{10}B concentration curves in low dose level and N_{max} values were defined at the peak value of the curves, respectively.

With these N_{th} and N_{max} data, the *CBE* factors were calculated by Equation (7) for all grade of brain tumor (**Figure 11**).

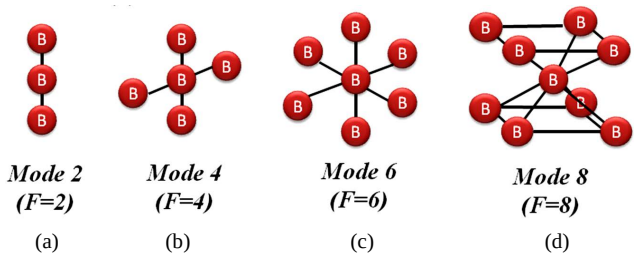

Figure 8. Typical intracellular distribution pattern of proximity *F*. (a) Dihedral; (b) Tetrahedron; (c) Hexahedron; (d) Octahedron.

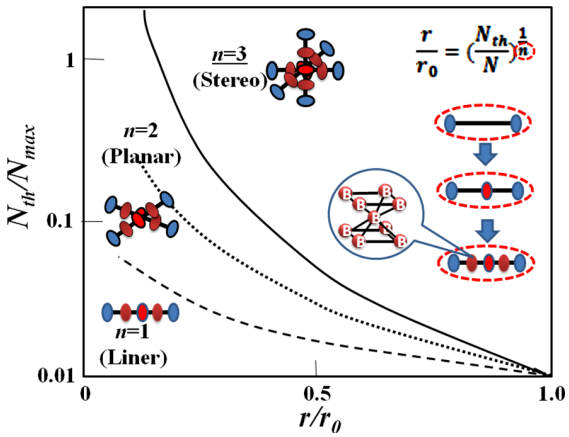

Figure 9. Intracellular cubic array of boron atom as a function of r/r_0.

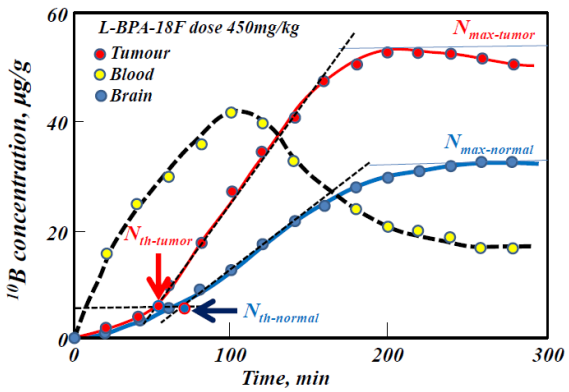

Figure 10. Typical change in ^{10}B concentration of brain tumour, blood and normal brain measured by dynamic PET technique.

From these results, it is found that all of these *CBE* factors on the lime of the *CBE* factor model in Equation (7), increases with tumor grade and categorized into three groups. These data were re-plotted to show more precise relationship between the *CBE* factor and tumor grade (**Figure 12**).

It is found that the *CBE* factors for AII and AIII vary widely whereas values for GBM display small variation and the same level of the *CBE* factor range of AIII.

After *BPA* administration, boron atoms are ingested into the cell model consisted of endoplasm and cell nucleus and Imahori reported [16] the kinetic analysis for these brain tumor patients by the Gjeddl-Patlak model [17] [18] using three-compartment rate constants (K_1, k_2 and k_3) (**Figure 13**).

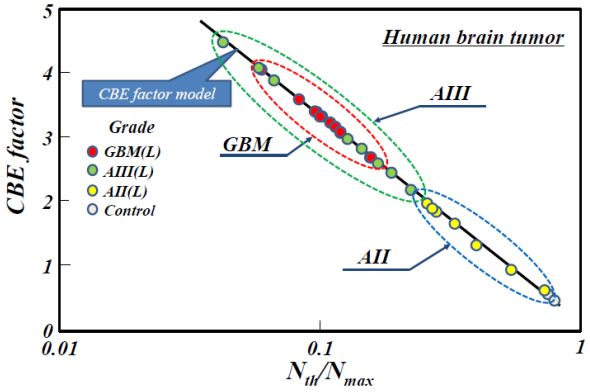

Figure 11. *CBE* factors calculated by *CBE* factor model in Equation (7) for three grade of brain tumour patients as a function of N_{th}/N_{max}.

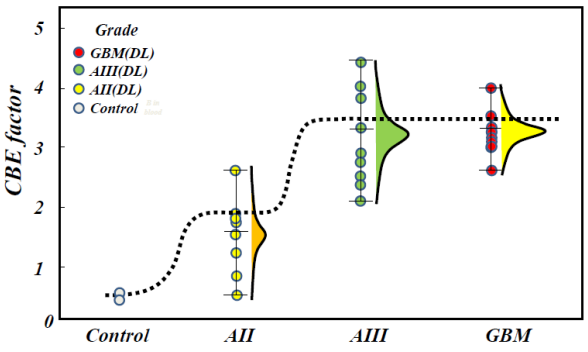

Figure 12. Distribution of the *CBE* factor range of brain tumour grade.

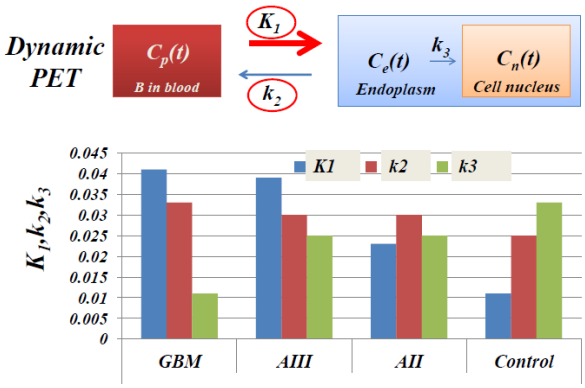

Figure 13. The rate constants of three compartment model for 33 brain tumor patients.

From the results, it is found that rate constant K_1 into cell increases drastically as tumor grade proceeding, whereas k_3 into cell nucleus decreases. This result means that the damage on toughness of these membranes deteriorates blocking capability and retention of *BPA* in cells due to attack of tumor to membrane of cell and nucleus, especially in GBM [16].

This fact indicated that the effectiveness of *BNCT* treatment achieves improvement in the brain tumor patients of grade AII and AIII, however its effectiveness is saturated for the grade of GBM.

3.4. Application of the Calculation Method and Its Clinical Significance

Normally, cancer patients are given low doses of intravenous radioactively-labelled 18F-*BPA* before *BNCT* and diagnosed cancer by Positron-Emission-Tomography (PET). Physicians developed a treatment plan by *BNCT* based on PET diagnosis and then after administrates high dose of *BPA* to the patients.

In present paper, we emphasized existence of N_{th} and showed a calculation method of the *CBE* factor with N_{th}/N_{max} in caption (2.1). Here, the most important thing for this calculation run is how to determined N_{th} and N_{max} values, and we presented N_{th} and N_{max} determination method in the case of brain tumor measured by dynamic PET technique in caption (2.3).

In practical use of this calculation method, 18F-*BPA* and *BPA* two-in-one medical mixture should be administrated into body and a small increment change of *BPA* concentration in tumor and normal tissue should be measured by dynamic PET technique simultaneously, as shown in the **Figure 10**. Then, N_{th} and N_{max} for tumor and normal tissue can be determined respectively, and the *CBE* factors for tumor and normal tissue can be defined by the calculation formula in Equation (7).

4. Conclusions

In present study, deterministic parsing model of the *CBE* factor for intracellular ^{10}B distribution was proposed in the following equation and at pretty much the same values as original CBE factor were obtained by the calculation to the original *CBE* factors for normal tissues and tumor by iteration calculation technique.

$$CBE = CBE_0 + \frac{F}{2}\left(1-\left(\frac{N_{th}}{N_{max}}\right)^{\frac{1}{n}}\right)\left\{2-\left(\frac{N_{th}}{N_{max}}\right)^{\frac{2}{n}}+\left(\frac{N_{th}}{N_{max}}\right)^{\frac{1}{n}}\right\} 0 < \frac{N_{th}}{N_{max}} < 1$$

In this equation, constants values of CBE_0, F and n are key factors for well-understanding of ^{10}B structural distribution in the cells analytically derived as 0.5,8 and 3 respectively in present study.

This *CBE* factor model was applied to human tumor brain cases and derived good results dovetailed with empirical facts.

References

[1] Bayanov, B., Belov, V., Kindyuk, V., Oparin, E. and Taskaev, S. (2004) Lithium Neutron Producting Target for BINP Accelerator-Based Neutron Source. *Applied Radiation and Isotopes*, **61**, 817-821. http://dx.doi.org/10.1016/j.apradiso.2004.05.032

[2] Willis, C., Lenz, J. and Swenson, D. (2008) High-Power Lithium Target for Accelerator-Based BNCT. *Proceedings of LINAC*08, Victoria, MOP063, 223-225.

[3] Halfon, S., Paul, M., Arenshtam, A., Berkovits, D., Bisyakoev, M., Eliyahu, I., Feinberg, G., Hazenshprung, N., Kijel, D., Nagler, A. and Silverman, I. (2011) High Power Accelerator-Based Boron Neutron Capture with a Liquid Lithium Target and New Applications to Treatment of Infections Diseases. *Applied Radiation and Isotopes*, **69**, 1654-1656. http://dx.doi.org/10.1016/j.apradiso.2011.03.016

[4] Ishiyama, S., Baba, Y., Fujii, R., Nakamura, M. and Imahori, Y. (2012) *In-Situ* Vacuum Deposition Technique of Lithium on Neutron Production Target for BNCT. *Nuclear Instruments and Methods in Physics Research*, **B288**, 18-22. http://dx.doi.org/10.1016/j.nimb.2012.07.024

[5] Ishiyama, S., Baba, Y., Fujii, R., Nakamura, M. and Imahori, Y. (2012) Synthesis of Lithium Nitride for Neutron Producton Target of BNCT by *In-Situ* Lithium Deposition and Ion Implantation. *Nuclear Instruments and Methods in Physics Research*, **B293**, 42-47. http://dx.doi.org/10.1016/j.nimb.2012.09.016

[6] Coderre, J.A., Morris, G.M., Micca, P.L., Fishe, C.D. and Ross, G.A. (1995) Comparative Assessment of Single-Dose and Fractional Boron Neutron Capture Therapy. *Radiation Research*, **166**, 310-317. http://dx.doi.org/10.2307/3578951

[7] Bath, R.F., Soloway, A.H., Goodman, J.H., Gahbauer, R.A., Gupta, N., Blue, T.E., Yang, W. and Tjarks, W. (2004) Boron Neutron Capture Therapy of Brain Tumors: An Merging Therapeutic Modality 2. *Neyrosurgery*, **44**, 433-451.

[8] Coderre, J.A. and Morris, G.M. (1999) The Irradiation Biology of Boron Neutron Capture Therapy. *Radiation Research*, **151**, 1-18. http://dx.doi.org/10.2307/3579742

[9] Morrsi, G.M., Coderre, J.A., Hopewell, J.W., Micca, P.L. and Rezvani, M. (1994) Response of the Skin to Boron Neutron Capture Therapy with p-Boronopenylalanine or Borocaptate Sodium. *Radiotherapy & Oncology*, **39**, 253-259.

[10] Fukuda, H., Kobayashi, T., Hiratsuka, J., *et al*. (1989) Estimation of Absorbed Dose in the Covering Skin of Human Melaoma Treated by Boron Capture Therapy. *Pigment Cell Research*, **2**, 365-369. http://dx.doi.org/10.1111/j.1600-0749.1989.tb00222.x

[11] Kiger, J.L., Kiger III, W.S., Riley, K.J., Binns, P.J., Patel, H., Hopewell, J.W., Harling, O.K., Busse, P.M. and Coderre, J.A. (2008) Functional and Histological Changes in Rat Lung after Boron Neutron Capture Therapy. *Radiation Research*, **171**, 60-69. http://dx.doi.org/10.1667/RR1266.1

[12] Suzuki, M., Masunaga, S., Kinachi, Y., Takagai, M., Sakurai, Y., Kobayashi, T. and Ono, K. (2000) The Effects of Boron Neutron Capture Therapy on Liver Tumors and Normal Hepatocytes in Mice. *Japanese Journal of Cancer Research*, **91**, 1058-1064. http://dx.doi.org/10.1111/j.1349-7006.2000.tb00885.x

[13] Morris, G.M., Smith, D.R., Patel, H., *et al*. (2000) Boron Microlocalization in Oral Mucosal Tissue. *British Journal of Cancer*, **82**, 1764-1771. http://dx.doi.org/10.1054/bjoc.2000.1148

[14] Horiguchi, H., Nakamura, T., Kumada, H., Yanagie, H., Suzuki, M. and Sagawa, H. (2011) Investigation of Irradiation Conditions for Recurrent Breast Cancer in JRR-4. *Applied Radiation and Isotopes*, **69**, 1882-1884. http://dx.doi.org/10.1016/j.apradiso.2011.03.036

[15] Ulmer, W. (2014) A New Calculation Formula of the Nuclear Cross-Section of Therapeutic Protons. *International Journal of Cancer Therapy and Oncology*, **2**, 1-13. http://dx.doi.org/10.14319/ijcto.0202.11

[16] Imahori, Y., Ueda, S., Ohmori, Y., *et al*. (1998) Fluorine-18-Labeled Fluoroboronophenylalanine PET in Patients with Glioma. *Journal of Nuclear Medicine*, **39**, 325-333.

[17] Wienhard, K., Herholz, K., Coenen, H.H., *et al*. (1991) Increased Amino Acid Tarransport into Brain Tumors Measured by PET of L-(2-18F) Fluorotyrosine. *Journal of Nuclear Medicine*, **32**, 1338-1346.

[18] Patlak, C.S., Blasberg, R.G. and Fenstmacher, J.D. (1983) Graphical Evaluation of Blood-to-Brain Transfer Constants from Multiple-Time Uptake Data. *Journal of Cerebral Blood Flow & Metabolism*, **3**, 1-7. http://dx.doi.org/10.1038/jcbfm.1983.1

Scientific Research Publishing (SCIRP) is one of the largest Open Access journal publishers. It is currently publishing more than 200 open access, online, peer-reviewed journals covering a wide range of academic disciplines. SCIRP serves the worldwide academic communities and contributes to the progress and application of science with its publication.

Other selected journals from SCIRP are listed as below. Submit your manuscript to us via either submit@scirp.org or Online Submission Portal.